

**Brief rhBMP-2 Treatment of Glucocorticoid-inhibited MC3T3-E1
Osteoblasts Rescues Commitment-Associated Cell Cycle and
Mineralization without Alteration of Runx2**

**Cynthia A. Luppen^{1,2}, Nathalie Leclerc^{1,2}, Tommy Noh¹, Artem Barski¹,
Arvinder Khokhar¹, Adele L. Boskey³, Elisheva Smith⁴ and Baruch Frenkel^{1,4}**

**Departments ¹Biochemistry & Molecular Biology⁴Orthopaedic Surgery
Institute for Genetic Medicine
Keck School of Medicine of the University of Southern California
Los Angeles, CA 90033**

**³Mineralized Tissues Research Laboratory
Hospital for Special Surgery
New York, NY 10021**

Running title: BMP-2 rescues mineralization without alteration of Runx2

**Funding sources: National Institutes of Health (AR47052, AR037661, DE04141 and
DE07211) and the Arthritis Foundation**

Address correspondence to:

**Baruch Frenkel
Institute for Genetic Medicine
University of Southern California Keck School of Medicine
2250 Alcazar Street, CSC/IGM240
Los Angeles, California 90033**

TEL: (323) 442-1322 FAX: (323) 442-2764 E-mail: frenkel@usc.edu

²These two authors contributed equally to the work

SUMMARY

Glucocorticoids (GCs) inhibit bone formation *in vivo*. In MC3T3-E1 osteoblasts, chronic administration of 1 μ M dexamethasone (DEX) starting at confluency results in >98% inhibition of bone morphogenetic protein-2 (BMP-2) expression and apatite mineral deposition. Here, it is shown that brief exposure to recombinant human BMP-2 (rhBMP-2), as short as 6 hours, is sufficient to induce irreversible commitment to mineralization in DEX-treated cultures. rhBMP-2 dose dependently rescued mineralization but not collagen accumulation in DEX-inhibited cultures. The selective restoration of mineralization was evident in the higher mineral-to-matrix ratios of DEX/rhBMP-2 co-treated cultures compared to control. We tested the involvement of the runt-related transcription factor 2 (Runx2) in the DEX inhibition and rhBMP-2 rescue of mineralization. Surprisingly, DEX did not decrease Runx2 DNA-binding activity, transactivation or association with the endogenous osteocalcin gene promoter. Furthermore, the rhBMP-2 rescue did not involve Runx2 stimulation, suggesting an important role for factors other than Runx2 in BMP-2 action. Finally, we studied the differentiation-related cell cycle, which persists during commitment to mineralization in untreated cultures, but is inhibited along with mineralization in DEX-treated cultures. Although both rhBMP-2 alone and DEX alone were antimitogenic, rhBMP-2 stimulated this cell cycle in DEX-inhibited cultures. In conclusion, brief rhBMP-2 treatment restores mineralization in DEX-inhibited MC3T3-E1 osteoblasts *via* a mechanism different from Runx2 stimulation. This restoration may be functionally related to the accompanying rescue of the differentiation-related cell cycle. The efficacy of short term BMP-2 treatment supports the potential of short-lived BMP vectors for skeletal therapy in both traditional and gene therapeutic approaches.

INTRODUCTION

Glucocorticoids (GCs) are potent anti-inflammatory agents for the treatment of diseases such as rheumatoid arthritis, systemic lupus erythematosus, asthma and some types of cancer. A major side effect of GC treatment is rapid bone loss and increased risk for fracture (1). The chief mechanism underlying bone loss during long-term GC treatment is impairment of bone formation (2-4). In addition to inducing bone loss, GCs have been shown to impede fracture healing in animal models (5,6), potentially via molecular mechanisms partly shared with GC-induced osteoporosis. Diverse cellular and molecular mechanisms contribute to GC-mediated inhibition of osteoblastic bone formation (reviewed in (3,4), including: (a) Attenuation of osteoblast proliferation (7-10) and especially of a differentiation-related cell cycle (11,12); (b) Promotion of osteoblast apoptosis (2); (c) Abrogation of collagen metabolism (13,14); (d) Inhibition of growth factors, such as IGF-I and BMP-2 (15,16); and (e) Inhibition of the osteoblast master transcription factor Runx2, also known as Cbfa1 and AML3 (17).

Investigation of the adverse effects of GCs on osteoblasts has been hampered by the positive actions of these same agents, which are primarily seen *in vitro*. In some isolated osteoblast cultures, the positive versus the negative effects occur at physiological versus pharmacological concentrations, respectively (18). However, many investigators have observed positive effects *in vitro* even with pharmacological GC concentrations (19-21). The present study utilizes the MC3T3-E1 osteoblast culture system, under conditions that support differentiation, evidenced by the robust deposition of bone-like collagenous

matrix with crystalline apatite (11,16). Moreover, in these cultures, administration of the synthetic GC dexamethasone (DEX) at pharmacological concentrations of 0.1-1 μ M strongly inhibits collagen accumulation and mineralization (11,16). We have previously shown that the DEX inhibition of mineralization occurs only during a commitment stage that is characterized by a cobblestone culture morphology and a uniquely controlled cell cycle (12). Additionally, DEX inhibits this commitment-associated cell cycle possibly revealing a mechanism for the DEX inhibition of nodule formation and mineralization (11,16).

Bone morphogenetic proteins (BMPs) are potent promoters of osteoblast differentiation and bone formation (22-26). Recombinant human BMP-2 (rhBMP-2) has been shown to overcome the inhibitory action of prednisolone on fracture healing (27). We have recently demonstrated that the DEX-mediated arrest of MC3T3-E1 osteoblast differentiation is associated with strong inhibition of endogenous BMP-2 gene expression (16). This inhibition appears to play a pivotal role in the overall adverse effect of GCs because administration of exogenous rhBMP-2 along with DEX counteracted the inhibitory effect of DEX on mineralization (16). However, nodule formation, characteristic of osteoblast differentiation *in vitro*, was not rescued by rhBMP-2 in the DEX-inhibited cultures (16). Furthermore, although collagen mRNA was induced by rhBMP-2 in the DEX-treated cultures, the DEX inhibition of extracellular collagen fibril accumulation was not reversed by rhBMP-2 (16).

The inhibitory effect of GCs on mineralization in MC3T3-E1 cultures is reversible (11). Therefore, we began the present study by asking if rhBMP-2 could rescue mineralization in DEX-treated cultures when administered after DEX. Also, because GCs cannot inhibit

mineralization when administered after the commitment stage described above, we asked if brief rhBMP-2 exposure of chronically DEX-treated cultures could elicit a commitment process sufficient for mineralization. Furthermore, we asked if a rescue mediated by brief exposure to rhBMP-2 is associated with recapitulation of the commitment-associated cell cycle as observed in untreated cultures. Additionally, because GCs inhibit Runx2 in calvarial and bone marrow stromal osteoblast cultures (17,28), and because BMPs induce Runx2 (29,30), we tested the involvement of this osteoblast master transcription factor in the rhBMP-2 rescue. We report that brief exposure to rhBMP-2 indeed restores both a differentiation-related cell cycle and mineralization in GC-treated MC3T3-E1 cultures. Moreover, both the cell cycle and mineralization are rescued even when exposure to rhBMP-2 commences after DEX treatment has begun. Surprisingly, the rhBMP-2 rescue is not associated with increased Runx2 activity.

EXPERIMENTAL PROCEDURES

Reagents – To maintain the MC3T3-E1 cell line, -minimum essential medium and penicillin/streptomycin were obtained from Invitrogen Corporation (Carlsbad, CA, USA). Individual lots of fetal bovine serum, also from Invitrogen, were selected based on their ability to support mineralization. The lot used in the current study was somewhat less osteogenic than that used in our recent study (16), resulting in delayed mineralization of the control cultures (day 14 versus day 10 in our recent study), as well as, possibly, stimulation of the control cultures by rhBMP-2. Ascorbic acid, -glycerophosphate and dexamethasone were from Sigma Co. (St. Louis, MO, USA). rhBMP-2 was generously provided by Wyeth Research (Cambridge, MA, USA). Cell culture dishes were purchased from Corning Incorporated (Corning, NY, USA). The biochemical assays were conducted using Sigma Diagnostics Kit 587 for calcium, Sigma Diagnostics Kit 104-LL for alkaline phosphatase, diaminobenzoic acid (DABA) for DNA (Sigma Chemical), and MicroBCA (Pierce Biochemical, Rockford, IL, USA) for protein. The histological calcium assay was conducted with Alizarin Red (Sigma). Runx2 antibodies for electromobility supershift assays were from Oncogene Research (San Diego, CA, USA). [-32P]ATP for probe labeling was from Amersham (Amersham Biosciences Corp, Piscataway, NJ, USA). Runx2 antibodies (sc-10758X), preimmune rabbit IgG and protein A/G Plus agarose beads for chromatin immunoprecipitation (ChIP) were from Santa Cruz Biotechnology (Santa Cruz, CA, USA). The protein A/G agarose beads were preblocked with 1 mg/ml salmon sperm DNA and 1 mg/ml BSA prior to use in the ChIP assays. Luciferase assay system was purchased from Promega Corporation (Madison, WI, USA). Luciferase constructs based on osteocalcin promoter sequences were

generously provided by Dr. Gerard Karsenty (Baylor College of Medicine, Houston, TX, USA). For cell cycle analysis, propidium iodide and Ribonuclease A were obtained from Sigma.

Cell culture – A robustly mineralizing subclone of the MC3T3-E1 cell line that has been previously described was used in this study (11). Cells were plated at 30,000 cells/cm² in 12 well plates for histological and biochemical assays, 6 well plates for transfection and 100 mm plates for cell cycle, Fourier Transform Infrared Spectroscopy (FTIR), Northern, RT-PCR, electromobility shift and chromatin immunoprecipitation experiments. Cells were maintained in α -minimum essential medium supplemented with 10% fetal bovine serum and 1.5% penicillin/streptomycin. Starting at 80% confluency (typically day 3, after plating on day 0), the culture medium was supplemented with 50 μ g/ml ascorbic acid and 10 mM β -glycerophosphate. In some experiments that are not shown, calcium deposition was measured in DEX-treated cultures after brief or chronic exposure to rhBMP-2, all in the presence of 5 mM instead of 10 mM β -glycerophosphate, and the results were essentially unchanged.

Histological demonstration of calcium deposition – Culture wells were washed once in phosphate-buffered saline (PBS) and fixed for one hour at 4°C in 70% ethyl alcohol. Calcium deposits were stained for 10 minutes at room temperature with Alizarin Red solution (40 mM, pH 4.2) that was filtered through Whatman paper prior to application. Non-specific staining was removed by several washes in water.

Biochemical Assays – Extracts for biochemical assays were collected by scraping the contents of each well in a 10 mM Tris-Saline buffer (pH 7.2) containing 0.2% Triton X-100. The extracts were tested for alkaline phosphatase activity using p-nitrophenyl phosphate as substrate. To measure calcium and DNA, aliquots of the extracts were acid-hydrolyzed (final concentration 0.5 N HCl) prior to processing. The spectrophotometric analyses of the protein (562 nm), ALP (410 nm) and calcium (575 nm) assays were conducted in 96-well plates using a PowerWave_x microplate scanning spectrophotometer (Biotek Instruments, Winooski, VT, USA). The fluorometric DNA assay was conducted using DABA essentially according to a published protocol (31), using excitation wavelength 400 ± 15 nm and emission wavelength 485 ± 10 nm on a FLx800 fluorescence microplate reader (Biotek Instruments).

Fourier Transform Infrared Spectroscopy (FTIR) – Extracellular matrix composition was analyzed by FTIR. Cell layers were collected in ammoniated water (50 mM ammonium bicarbonate, pH 8.0), lyophilized and analyzed as potassium bromide (KBr) pellets on a BioRad FTS 40-A spectrometer (BioRad, Cambridge, MA, USA). The spectral data were baseline corrected and analyzed using GRAMS/386 software (Galactic Industries, Salem, NH, USA) as previously described (32). The mineral-to-matrix ratio was derived from the areas of phosphate (900 to 1200 cm^{-1}) and protein amide I (1585 to 1720 cm^{-1}) absorbance. Crystallinity, or crystal maturity, was evaluated based on the intensity ratios of the $1030:1020$ sub-bands of the phosphate ν_1, ν_3 absorbance spectrum (33). The presence of crystalline apatite was verified by a split phosphate ν_2 band (500 to 635 cm^{-1}).

RNA analyses – Total cellular RNA was isolated using TRIzol Reagent (Invitrogen) and osteocalcin gene expression was evaluated as previously described (16). For Northern analysis, 15 µg of total RNA was separated in a 1% agarose-formaldehyde gel, transferred onto Hybond-N+ membrane (Amersham) and hybridized with a 300-bp mouse osteocalcin probe excised from pBGP with *Bam*HI and *Eco*RI. Prehybridization and hybridization were performed in 50 mM sodium phosphate buffer (pH 7.4) containing 50% formamide, 5X SSC, 10X Denhardt's solution, 1% SDS and 0.1 mg/ml denatured salmon sperm DNA. The blots were washed extensively in buffer containing 2X SSC and 0.1% SDS at room temperature and then at 50°C and exposed to film overnight. For reverse transcriptase-polymerase chain reactions (RT-PCR), single-stranded cDNA was synthesized from the Trizol-extracted, DNase-treated RNA. A 187-bp osteocalcin cDNA fragment was PCR amplified as described previously under conditions providing close-to-linear signal as a function of input (16).

Runx2 Electromobility Shift Assay (EMSA) – Cultures for whole cell extract preparation were washed with PBS, and the cell layers were scraped and centrifuged at 3000 rpm for 5 minutes at 4°C. Cell pellets were resuspended in 1.5 packed cell volumes of lysis buffer (100 mM Hepes pH 7.5, 500 mM KCl, 5 mM MgCl₂, 0.5 mM EDTA, 28% glycerol) containing protease and phosphatase inhibitors (5 mM NaF, 0.1 mM Na₃VO₄, 5 µg/ml aprotinin, 5 µg/ml leupeptin, 1 mM DTT, 1 mM PMSF and 20 µM MG132). The cells were further subjected to successive passes through 18.5, 20.5 and then 23 gauge needles, followed by centrifugation at 14,000 rpm for 30 minutes at 4°C to remove cell debris. The supernatant was snap frozen and stored at –80°C. EMSA was performed

with 15 µg whole cell extract and 80 fmoles of an end-labeled 23 base pair oligonucleotide probe containing the Runx2-binding OSE2 site from the mouse osteocalcin gene 2 (OG2) promoter (34). The cell extract was initially preincubated on ice for 10 minutes in the presence of 100 mM KCl with 1 µg salmon sperm DNA and, when indicated, unlabeled oligonucleotides or antibodies. Probe binding reaction (final volume: 20 µl) was then performed in 20 mM Hepes buffer (pH 7.5) containing (final concentrations) 50 mM KCl, 1 mM MgCl₂, 2 mM EDTA and 2.8% glycerol for 10 minutes on ice followed by 15 minutes at room temperature. The protein-DNA complexes were then resolved in 0.25X TBE native polyacrylamide (5%) gel containing 5% glycerol.

Transient transfection and Luciferase assay – MC3T3-E1 cells were plated as above (day 0) and transiently transfected on day 1 using calcium phosphate co-precipitation as described previously (11). DEX (1 µM) and/or rhBMP-2 (100 ng/ml) treatment commenced as cultures became confluent on day 4 and lasted 48 hours. Cells were then lysed and luciferase activity was determined using an MLX microtiter plate luminometer (Dynex Technologies, Chantilly, VA, USA).

Chromatin Immunoprecipitation (ChIP) – ChIP was performed essentially as previously described (35). Crosslinking was performed using 1% formaldehyde (10 min, 25°C) and was stopped by adding glycine to a final concentration of 0.125 M. Cells were swelled in hypotonic buffer: 10 mM HEPES, 10 mM KCl, 1.5 mM MgCl₂ and protease inhibitor cocktail (Complete mini, Roche Applied Science, Indianapolis, IN, USA). Nuclei were

lysed in 50 mM Tris-HCl buffer (pH 8.1) containing 1% SDS, 10 mM EDTA and protease inhibitors. Resulting chromatin solution was sonicated using a Virsonic 60 sonicator (VirTis Company, Gardiner, NY, USA; 4 pulses at 4 watts, 10 sec each) and centrifuged at 16,000g for 10 min to remove cell debris. At this point, samples were diluted to adjust the absorbance to 0.25 OD₂₆₀ units and 100 µl was further diluted 10 times with IP buffer: 16.7 mM Tris-HCl (pH 8.1), 0.01% SDS, 1.1% Triton X-100, 1.2 mM EDTA, 167 mM NaCl and protease inhibitors. Preclearing was performed with 2 µg preimmune rabbit IgG and 100 µl of protein A/G agarose beads. Following overnight incubation with 10 µg Runx2 antibodies, complexes were precipitated with 30 µl of A/G agarose and the beads were sequentially washed with IP buffer, high salt buffer (0.1% SDS, 1% Triton X-100, 2 mM EDTA, 20 mM Tris-HCl pH 8.1, 500 mM NaCl), sarcosyl buffer (0.2% sarcosyl, 2 mM EDTA, 50 mM Tris-HCl pH 8.1) and TE. Complexes were eluted twice with 250 µl of elution buffer (1% SDS, 0.1M NaHCO₃) and crosslinks were reversed by incubation at 65 °C for 4 hours. The DNA was then deproteinized and purified on QIAquick PCR purification column (Qiagen, Valencia, CA, USA). The osteocalcin -264/-7 promoter fragment was amplified with the primers 5'-gagagcacacagtaggagtggtggag and 5'-tccagcatccagtagcatttatatcg. The insulin -246/-4 promoter fragment was amplified as a negative control with the primers 5'-tggatgcccaccagctttatagtcc and 5'-aactggttcacaggccatctggtc. PCR reactions were performed within a close-to-linear range under conditions that yield comparable signals for osteocalcin and insulin when genomic DNA is used as template.

Cell cycle analysis – Cell cycle profiles were determined as previously described (11). Briefly, cells were trypsinized and collected by centrifugation (4000 rpm, 4° C, 15 min) in phosphate-buffered saline. Following centrifugation, the cells were resuspended in 100% ethyl alcohol and kept at –20° C. The ethyl alcohol was removed by centrifugation (4000 rpm, 4° C, 15 min) and the cells were resuspended in Hank’s balanced buffer solution containing 20 µg/ml of propidium iodide and 100 µg/ml DNase free-Ribonuclease A. Following 30 minute incubation at room temperature, the stained cells were analyzed by flow cytometry using the EPICS XL-MCL analyzer (Beckman Coulter, Fullerton, CA, USA) and the percentages of cells in the G1, S and G2/M phases of the cell cycle were determined using MultiCycle analysis software (Phoenix Flow Systems, San Diego, CA, USA).

Statistical Analysis – Results from each quantitative assay were analyzed in order to test four effects: (i) the effect of DEX in the absence of BMP-2; (ii) the effect of BMP-2 in the absence of DEX (iii) the effect of BMP-2 in the presence of DEX and (iv) the effect of chronic versus brief rhBMP-2 treatment for each condition. Means and standard deviations were compared using the Student’s t-test and the differences were considered significant when $p \leq 0.05$.

RESULTS

Inhibition of mineralization by chronic DEX treatment is corrected by chronic BMP-2 treatment commencing 48 hours after DEX. We have previously shown that rhBMP-2 counteracts GC-mediated inhibition of mineralization in MC3T3-E1 osteoblast cultures (16). In this study the negative regulator, DEX, and the positive regulator, rhBMP-2, were administered together commencing on day 3. The ability of rhBMP-2 to rescue mineralization in cultures that have already been exposed to DEX for a substantial period of time was not tested. Therefore, in the current study, MC3T3-E1 cells were treated with DEX starting on day 3 and rhBMP-2 was added 48 hours later (day 5). DEX and rhBMP-2 treatments continued throughout the rest of the experiment. Analysis of calcium deposition on day 14, by either Alizarin red staining (Figure 1A) or biochemical assay (Figure 1B), showed that 1 μ M DEX completely inhibited mineralization while rhBMP-2, at either 10 or 100 ng/ml, dramatically counteracted the DEX inhibition. A time course experiment (Figure 1B) revealed that the rhBMP-2-rescued mineralization was even accelerated as compared to that of control cultures. Furthermore, FTIR analysis of day 14 cultures showed that the crystallinity of the rescued mineral was comparable to that of control; the 1030:1020 phosphate sub-band ratios ranged between 1.057 and 1.068 in the control cultures and between 1.051 and 1.088 in the cultures rescued with either 10 ng/ml or 100 ng/ml of rhBMP-2. Thus, rhBMP-2 not only counteracts DEX when the two are administered together (16), but it also rescues deposition of apatite-like mineral when added 48 hours following commencement of DEX treatment.

GC-inhibited cultures are rescued by brief exposure to BMP-2. Maximum inhibition of mineralization in MC3T3-E1 cultures is observed when DEX treatment commences just prior to confluency (day 3) (11). During the 1-3 days that follow confluency, cultures become resistant to the inhibitory effects of DEX which indicates a process of commitment to mineralization (11). If rhBMP-2 induces such a commitment, then the rescue of the DEX-treated cultures might not require chronic administration of rhBMP-2. To test this possibility, we chronically treated MC3T3-E1 cells with DEX from day 3-14, and limited the treatment with 100 ng/ml rhBMP-2 to brief exposure on day 5. The brief rhBMP-2 exposure lasted between 15 minutes and 12 hours, following which the cultures were maintained in the presence of DEX and stained with Alizarin red on day 14. As shown in Figure 2A, four hours of rhBMP-2 treatment on day 5 was sufficient to induce commitment to mineralization and full commitment was achieved after six hours. Although both doses of rhBMP-2, 10 and 100 ng/ml, were equally effective in rescuing mineralization when administered chronically (Figure 1), this was not the case for brief exposure. As demonstrated in Figure 2B by Alizarin red staining and in Figure 2C by a biochemical assay, ten-hour exposure of DEX-treated cultures to 10 ng/ml rhBMP-2 induced only marginal calcium accumulation, whereas the 100 ng/ml dose fully rescued mineralization (Figures 2B,C). A time course experiment monitoring calcium deposition following brief exposure to rhBMP-2 revealed that the rescued mineralization was accelerated compared to control cultures (Figure 2C).

The nature of the rescued mineral was evaluated by FTIR. As shown by representative spectra, both the control and the rescued cultures formed crystalline apatite, as indicated

by the split phosphate ν_2 band (III in Figure 2D). Despite some apparent differences in crystal structure between the rescued and the control mineral (the rescued mineral phosphate ν_2 band was sharper and more reminiscent of a bone-like extracellular matrix), the crystallinity, measured as the intensity ratio between the 1030 and 1020 phosphate sub-bands, was comparable between the rescued (range: 1.064 - 1.085) and the control mineral (range: 1.051 - 1.088).

Rescue of mineralization by chronic or brief exposure to BMP-2 is not accompanied by rescue of DEX-inhibited collagen accumulation or nodule formation. In our previous study, rhBMP-2 did not counteract the DEX inhibition of collagen accumulation or nodule formation (16). Because rhBMP-2 alone inhibited collagen accumulation (16), we postulated that delayed or brief rhBMP-2 administration might better support collagen accumulation and nodule formation. Cultures were treated with DEX starting on day 3 and then with rhBMP-2 starting on day 5, for either ten hours or nine days. Collagen and DNA were measured on day 6-14. Figure 3A describes the accumulation of collagen, corrected for DNA as a measure of cell number. DEX inhibited collagen accumulation by 82-95% compared to control at all time points, while DNA accumulation was inhibited by only 14-32% (Figure 3A, bottom panel). Unlike the mineralization results, neither chronic nor brief administration of rhBMP-2 to the DEX-treated cultures rescued collagen accumulation to near-control levels at any time point. In fact, 100 ng/ml rhBMP-2, especially when administered chronically, further inhibited collagen accumulation on days 10 and 14 compared to DEX alone. A similar inhibition of collagen accumulation by rhBMP-2 was observed in the absence of DEX (Figure 3A).

We further studied the effects of DEX and/or rhBMP-2 administration on the properties of the extracellular matrix by FTIR analysis of day 14 cultures. DEX alone decreased the mineral-to-matrix ratio by 4-fold (Figure 3B), suggesting stronger inhibition of mineral deposition as compared to that of collagen accumulation. Chronic exposure of the DEX-treated cultures to rhBMP-2 (10 or 100 ng/ml) increased the mineral-to-matrix ratio to levels greater than control (Figure 3B), reflecting the rescue of calcium accumulation without an increase in collagen accumulation. Ten-hour exposure of the DEX-treated cultures to rhBMP-2 also increased the mineral-to-matrix ratio, but only at the 100 ng/ml dose (Figure 3B), consistent with the dose-dependent rescue of calcium accumulation when rhBMP-2 is administered for a short time (Figure 2C).

DEX treatment arrests MC3T3-E1 cultures at the cobblestone stage, preventing condensation and nodule formation (11,12). Co-administration of rhBMP-2 does not rescue nodule formation in DEX-treated cultures (16). Microscopic evaluation of day 10 cultures in the current study revealed that brief exposure of DEX-treated cultures to rhBMP-2 (on day 5) also failed to rescue nodule formation (Figure 3C). This was also the case in DEX-treated cultures chronically exposed to rhBMP-2 starting on day 5 (data not shown). Thus, both chronic and brief exposure of DEX-treated cultures to rhBMP-2 rescues mineralization, but collagen accumulation and nodule formation remain inhibited.

Sustained upregulation of Alkaline Phosphatase requires continuous treatment with BMP-2. We next examined alkaline phosphatase (ALP) activity in DEX-treated cultures

and those treated with rhBMP-2 either briefly or chronically. MC3T3-E1 cells were treated as above with DEX commencing on day 3, and with rhBMP-2 commencing on day 5, and ALP activity was measured one, five, or nine days following rhBMP-2 administration. Although treatment with rhBMP-2 generally induced ALP activity (Figure 4), this induction did not always parallel mineralization. Most notably, while brief exposure of DEX-treated cultures to 100 ng/ml rhBMP-2 was as effective in rescuing mineralization as was chronic treatment (Figures 1B and 2C), only the chronic treatment strongly induced ALP activity, reaching 7.5-fold stimulation on day 14, as compared to only 1.9-fold with brief treatment (Figure 4). Furthermore, while brief rhBMP-2 treatment rescued mineralization in a dose-dependent manner (Figure 2C), the two rhBMP-2 doses tested, 10 and 100 ng/ml, had similar effects on ALP activity (Figure 4). Finally, DEX itself, which completely abolished mineralization, did not inhibit, but in fact stimulated ALP activity in the present study (Figure 4). These results suggest that DEX and rhBMP-2 affect mineralization in MC3T3-E1 cultures via mechanisms different from those regulating ALP activity.

BMP-2 rescue of mineralization in MC3T3-E1 cultures is not accompanied by upregulation of Runx2 activity. Runx2 is a master transcription factor in osteoblast differentiation and mineralization. In primary rat calvarial osteoblasts and in the ST2 bone marrow-derived stromal cell line DEX down-regulates Runx2 (17,28). There is ample evidence for upregulation of Runx2 by BMP-2 (29,30). However, as demonstrated by EMSA in Figure 5A, Runx2 DNA-binding activity was not significantly altered in MC3T3-E1 cultures treated with DEX for up to 42 hours, by which time both osteocalcin

gene expression (Figure 5D) and the differentiation-related cell cycle (11) were strongly inhibited. Furthermore, Runx2 DNA-binding activity was not stimulated during a 10-hour exposure of DEX-treated cultures to 100 ng/ml rhBMP-2 (Figure 5B), which was sufficient for the rescue of mineralization (Figure 2A).

Because Runx2 activity may be modulated in ways that are not detectable by EMSA, the effects of DEX and rhBMP-2 on Runx2 were also tested by transfecting MC3T3-E1 cells with luciferase constructs that report on Runx2 transcriptional potential. As shown in Figure 6, neither DEX, nor rhBMP-2, nor the combination of both agents significantly affected luciferase activity driven by the osteocalcin 147 base pair (bp) proximal promoter. The dependence of this promoter activity on the Runx2-binding OSE2 site at position –138 (34) was confirmed in our MC3T3-E1 cells, as mutation of the OSE2 site resulted in 8-9 fold decrease in luciferase activity in both untreated and DEX-treated cells (data not shown). We further tested Runx2 transcriptional activity using the (OSE2)X6-luc construct, which contains six repeats of the OSE2 site fused upstream of the minimal 34-bp osteocalcin promoter (34). As expected, activity of (OSE2)X6-luc was several fold higher than that of –147 OC-luc, and mutations in the OSE2 repeats abolished activity (Figure 6). However, activity of the synthetic (OSE2)X6 enhancer was not significantly affected by DEX, rhBMP-2 or both together. Unlike both the 147 bp osteocalcin promoter and the synthetic OSE2 driven promoter, the 1.3-kb osteocalcin promoter was inhibited by DEX and partially rescued by rhBMP-2 (Figure 6), resembling the responsiveness of the endogenous osteocalcin gene (ref. 16 and Figure 6, inset). This data suggests that transcription factors binding upstream of position –147, likely other

than Runx2, mediate osteocalcin responsiveness to DEX and rhBMP-2 in MC3T3-E1 cells.

We also tested the possibility that Runx2 is involved in the GC-inhibition of mineralization in a way that cannot be disclosed by transient transfection assays. Specifically, we hypothesized that DEX blocks the accessibility of Runx2 to target genes within the nuclei of living cells. MC3T3-E1 cultures were treated with DEX during various stages of differentiation. DNA and DNA-binding proteins were cross-linked with formaldehyde and chromatin prepared from these cultures was immunoprecipitated with anti-Runx2 antibodies. The osteocalcin gene was used as a model Runx2 target. Occupancy of this gene by Runx2 was determined by PCR amplification of an osteocalcin promoter fragment in the immunoprecipitated DNA. Amplification of an insulin promoter fragment served as an internal negative control to measure the level of non-specific precipitation (background) for each ChIP. The results in Figure 7, representing one of 2-3 ChIPs for each treatment protocol, indicate that DEX did not reduce occupancy of the osteocalcin promoter by Runx2.

rhBMP-2 rescues differentiation-related cell cycle in DEX-treated MC3T3-E1 cultures. As differentiating MC3T3-E1 osteoblast cultures become confluent they assume cobblestone appearance then enter a commitment stage characterized by persistent cell cycle and condensation (11,12). DEX-mediated inhibition of mineralization is associated with parallel attenuation of this differentiation-related cell cycle (11,12). To test whether the rhBMP-2-rescue of mineralization (Figures 1,2) is

associated with rescue of the differentiation-related cell cycle, MC3T3-E1 cultures were treated with DEX and/or rhBMP-2 commencing on day 3 and 5, respectively, and cell cycle profiles were determined immediately following rhBMP-2 administration. The rhBMP-2 was administered either along with medium change as in Figure 1, or by addition without medium change, as in Figure 2. Cells were then collected every three hours until 37 hours. The effects of DEX and rhBMP-2 on cell cycle progression were independent of the method of rhBMP-2 addition (Figure 8). As reported previously (16), DEX and rhBMP-2 each inhibited the G1/S transition, indicated by approximately 2-fold decrease in the percentage of cells in the S phase of the cell cycle (Figure 8). However, the addition of rhBMP-2 to DEX-treated cultures resulted in rescue of the cell cycle, which reached near-control levels by 25 hours of rhBMP-2 treatment (Figure 8). Thus, rhBMP-2 concomitantly rescues both the differentiation-related cell cycle and the commitment to mineralization in GC-inhibited MC3T3-E1 cultures.

DISCUSSION

GCs inhibit proliferation, impede differentiation and induce apoptosis of both immune cells and osteoblasts, thus frequently causing osteoporosis as a side effect when administered for immune suppression. In the absence of synthetic GCs that specifically suppress immune cells, a search for compounds that protect osteoblasts from GCs is warranted. Here, we employ DEX-arrested MC3T3-E1 osteoblast cultures, and demonstrate that rhBMP-2 rescues mineralization, even when added 48 hours after DEX and only for a brief period of 4-6 hours. Furthermore, the rescued cultures have increased mineral-to-matrix ratios, their mineral is deposited as bone-like crystalline apatite, and calcium accumulation is accelerated as compared to control cultures not treated with DEX or rhBMP-2.

Local administration of rhBMP-2 has been demonstrated effective in counteracting the inhibitory effect of GCs on osteotomy healing in a rabbit model (27). In that study, administration of rhBMP-2 (on an absorbable collagen sponge) was both preceded and followed by systemic treatment with high-dose prednisolone. The present study sheds light on the remarkable efficacy of rhBMP-2 in the osteotomy healing model, because it demonstrates the ability of rhBMP-2 to counteract GCs when administered both following the commencement of GC treatment and for just a brief period of time. It is now easier to imagine how rhBMP-2 in the *in vivo* study could have induced irreversible commitment in cells of the chondro-osteoblast lineage at the osteotomy site, resulting in accelerated repair regardless of whether the rhBMP-2 itself was present during the entire

healing process. The concept of BMP-2-induced irreversible commitment is also important in the context of gene therapy: complex and long processes of cartilage and bone formation may be induced by vectors, genes or engineered cells producing BMPs, even if the vectors themselves are short-lived.

How long should rhBMP-2 be administered in order to induce commitment to mineralization in GC-treated osteoblasts? In the present study, detectable commitment of DEX-treated MC3T3-E1 cells to mineralization required more than one but less than four hours of exposure to 100 ng/ml rhBMP-2. Full commitment required approximately six hours. However, more than ten hours of rhBMP-2 treatment was required to induce commitment to mineralization using the lower, 10 ng/ml dose. In addition to dosage, we anticipate that rhBMP-2-induced commitment will depend on the developmental stage in which GCs are introduced to arrest differentiation. Likely, if cells are arrested after they have begun spontaneous commitment, then less rhBMP-2 (time or dose) will be required to induce full commitment.

Despite its efficacy in promoting fracture healing, rhBMP-2 is not yet a clinical option for the treatment of GC-induced osteoporosis because of its short half-life following systemic administration. Furthermore, in the *in vitro* MC3T3-E1 culture system, rhBMP-2 did not restore the entire osteoblast phenotype. Specifically, collagen accumulation remained inhibited by chronic DEX treatment regardless of whether rhBMP-2 administration paralleled that of DEX (16), or started 48 hours later than DEX and was administered for the remainder of the study or for a brief period of ten hours (this study).

Thus, although rhBMP-2 increases $\alpha 1(I)$ collagen mRNA levels (36,37) including in MC3T3-E1 cells (16), it is unable to counteract the post-transcriptional inhibitory effect of GCs on collagen synthesis. This post-transcriptional effect may be related to the general inhibition of translation by GCs, which has been documented primarily in myoblasts (38).

The opposing effects of DEX and rhBMP-2 on mineralization in the MC3T3-E1 culture model provide a unique opportunity to discover novel molecular mechanisms mediating the actions of these two ligands. Shortly after the discovery of Runx2, it was proposed, based on *in vitro* data (17,39), that GCs and BMPs exert opposing effects on osteoblast commitment by their respective inhibition and stimulation of Runx2 (40). In MC3T3-E1 cultures, we and others have previously shown that GCs, either at physiological or pharmacological concentrations, induce only modest alterations in the levels of Runx2 type I and type II mRNA (16), the level of the Runx2 protein and its DNA-binding activity (41). In the present study, we further demonstrate that pharmacological levels of GCs do not alter Runx2 DNA binding activity in early MC3T3-E1 cultures. Moreover, transfection experiments show that DEX does not alter Runx2-mediated transcription of the osteocalcin gene in these cells. Finally, using the osteocalcin promoter as a model Runx2 target gene, we demonstrate by ChIP that DEX does not impede Runx2 accessibility to its cognate elements in the chromatin of living MC3T3-E1 cells.

The lack of Runx2 inhibition in MC3T3-E1 cultures during the initial 42 hours of GC treatment is unlike the inhibition observed in fetal rat calvarial osteoblasts (feRCOBs)

(17). In later stages of MC3T3-E1 cultures, DEX decreased Runx2 DNA binding activity by up to 2-fold (data not shown). In early MC3T3-E1 cultures, the repression of endogenous osteocalcin gene expression and the inhibition of the transfected 1.3-kb osteocalcin promoter, without a decrease in Runx2, suggest that GCs inhibit additional, yet unidentified, transcription factor(s). The potential importance of such additional GC-responsive factors is underscored by another study with feRCOBs in which the GC-inhibition of Runx2 gene expression was not accompanied by inhibition of mineralization (42). Mapping the osteocalcin GC response element under conditions that mediate the strong phenotype suppression in MC3T3-E1 cells may lead to disclosure of the non-Runx2 inhibitory mechanism.

Just as GCs inhibited osteocalcin gene expression in early MC3T3-E1 cultures in a Runx2-independent fashion, BMP-2 restored osteocalcin expression without alteration of Runx2. Non-Runx2, BMP-2-responsive mechanisms have been previously implied when high doses of BMP-2 stimulated the osteocalcin promoter in Runx2 knockout cells (39) and recently *Dlx5* was reported to be a direct BMP-2 target that acts upstream of Runx2 during osteoblast differentiation (43). In the present study, Runx2 was not stimulated by up to ten hours of rhBMP-2 treatment, whereas a 6-hour treatment was sufficient to induce commitment to mineralization. Furthermore, rhBMP-2-stimulated osteocalcin transcription through an element(s) other than the Runx2 binding site, OSE2. Also, the rescue of mineralization did not parallel alkaline phosphatase activity, a classical target of BMPs. Factors other than Runx2 that mediate the BMP-2 rescue of mineralization in GC-treated MC3T3-E1 cultures may be disclosed in future investigations of the

combined actions of GCs and rhBMP-2 on both the distal osteocalcin promoter and the differentiation-related cell cycle, as explained in the next paragraph.

We previously defined a commitment stage during MC3T3-E1 osteoblast differentiation, which occurs as cells reach confluency (11). Morphologically, this commitment stage is characterized by transition from cobblestone to condensed cultures. We have further characterized this commitment based on its association with spontaneous upregulation of c-myc (12) and a uniquely controlled, post-confluent persistent cell cycle (11). This differentiation-related cell cycle is inhibited by GCs via activation of GSK3 β , leading to inhibition of c-myc expression (12) and ultimately downregulation of cyclin A, which then dissociates from E2F4/p130 complexes at the promoters of cell cycle regulatory genes (11). We presented several lines of evidence linking the differentiation-related cell cycle to mineralization: both were inhibited by GCs, both were reversible upon GC withdrawal and both were antagonized by the GC partial agonist/antagonist RU486 (11). In the present study we show that the rhBMP-2-induced commitment to mineralization is also associated with resumption of what appears to be a differentiation-related cell cycle. This cell cycle reached near-control levels in GC-treated osteoblasts within 25 hours of rhBMP-2 administration and was induced whether or not fresh serum was added along with the rhBMP-2 treatment. Moreover, it appears that induction of the differentiation-related cell cycle by rhBMP-2 in the DEX-treated cultures was quite specific, because: 1) rhBMP-2 did not stimulate, but in fact inhibited the cell cycle in cultures not treated with DEX, in which the differentiation-related cell cycle has likely been completed at the time of rhBMP-2 administration; 2) Despite the cell cycle rescue, the DEX/rhBMP-2-co-

treated cultures maintained a cobblestone morphology throughout the experiment, as demonstrated by the micrographs of day 10-cultures; and 3) In our previous study, cell cycle analysis of DEX/rhBMP-2-co-treated cultures under conditions different from those employed here, did not show cell cycle rescue, either because cells were collected too late (72 hours following administration of rhBMP-2) or because treatment with both agents was initiated at the same time (16). Ongoing investigations of the differentiation-related cell cycle and its regulation by DEX and rhBMP-2 may provide insight into novel mechanisms other than Runx2, which mediate the inhibition and stimulation of osteoblast differentiation by GCs and BMPs.

ACKNOWLEDGMENTS

The authors would like to acknowledge the excellent technical contributions of Sara Martinez, Lyudmila Spevak, and Yujiki Fujimoto. We are grateful to Wyeth Research for generously providing rhBMP-2. The osteocalcin probe and the osteocalcin promoter and (OSE2)X6 constructs were a generous gift from Gerard Karsenty (Baylor School of Medicine). C.A.L. was supported by training grant DE07211 from the National Institute of Dental and Craniofacial Research. This work was supported by grants from the National Institutes of Health (AR47052, AR037661 and DE04141) and from the Arthritis Foundation.

REFERENCES

1. Van Staa, T. P., Leufkens, H. G., Abenhaim, L., Zhang, B., and Cooper, C. (2000) *J Bone Miner Res* **15**, 993-1000
2. Weinstein, R. S., Jilka, R. L., Parfitt, A. M., and Manolagas, S. C. (1998) *J Clin Invest* **102**, 274-282
3. Canalis, E., and Delany, A. M. (2002) *Ann N Y Acad Sci* **966**, 73-81
4. Lukert, B. (1997) in *Osteoporosis* (Markus, R., Feldman, D., and Kelsey, J., eds), pp. 801-820, Academic Press, San Diego, CA
5. Waters, R. V., Gamradt, S. C., Asnis, P., Vickery, B. H., Avnur, Z., Hill, E., and Bostrom, M. (2000) *Acta Orthop Scand* **71**, 316-321.
6. Kostenszky, K. S., and Olah, E. H. (1974) *Acta Biol* **25**, 49-60
7. Chen, T. L., Cone, C. M., and Feldman, D. (1983) *Endocrinology* **112**, 1739-1745
8. Chevalley, T., Strong, D. D., Mohan, S., Baylink, D., and Linkhart, T. A. (1996) *Eur J Endocrinol* **134**, 591-601
9. Kamalia, N., McCulloch, C. A., Tenebaum, H. C., and Limeback, H. (1992) *Blood* **79**, 320-326
10. Lian, J. B., Shalhoub, V., Aslam, F., Frenkel, B., Green, J., Hamrah, M., Stein, G. S., and Stein, J. L. (1997) *Endocrinology* **138**, 2117-2127
11. Smith, E., Redman, R. A., Logg, C. R., Coetzee, G. A., Kasahara, N., and Frenkel, B. (2000) *J Biol Chem* **275**, 19992-20001
12. Smith, E., Coetzee, G. A., and Frenkel, B. (2002) *J Biol Chem* **277**, 18191-18197
13. Delany, A. M., Gabbitas, B. Y., and Canalis, E. (1995) *J Cell Biochem* **57**, 488-494
14. Delany, A. M., Jeffrey, J. J., Rydziel, S., and Canalis, E. (1995) *J Biol Chem* **270**, 26607-26612
15. Linkhart, T. A., Mohan, S., and Baylink, D. J. (1996) *Bone* **19**, 1S-12S.
16. Luppen, C. A., Smith, E., Spevak, L., Boskey, A. L., and Frenkel, B. (2003) *J Bone Miner Res* **18**, 1186-1197
17. Chang, D. J., Ji, C., Kim, K. K., Casinghino, S., McCarthy, T. L., and Centrella, M. (1998) *J Biol Chem* **273**, 4892-4896
18. Ishida, Y., and Heersche, J. N. (1998) *J Bone Miner Res* **13**, 1822-1826
19. Tenenbaum, H. C., and Heersche, J. N. (1985) *Endocrinology* **117**, 2211-2217
20. Leboy, P. S., Beresford, J. N., Devlin, C., and Owen, M. E. (1991) *J Cell Physiol* **146**, 370-378
21. Shalhoub, V., Conlon, D., Tassinari, M., Quinn, C., Partridge, N., Stein, G. S., and Lian, J. B. (1992) *J Cell Biochem* **50**, 425-440
22. Urist, M. R. (1965) *Science* **150**, 893-899.
23. Wozney, J. M., Rosen, V., Celeste, A. J., Mitsock, L. M., Whitters, M. J., Kriz, R. W., Hewick, R. M., and Wang, E. A. (1988) *Science* **242**, 1528-1534.
24. Wang, E. A., Rosen, V., Cordes, P., Hewick, R. M., Kriz, M. J., Luxenberg, D. P., Sibley, B. S., and Wozney, J. M. (1988) *Proc Natl Acad Sci U S A* **85**, 9484-9488.
25. Gitelman, S. E., Kobrin, M. S., Ye, J. Q., Lopez, A. R., Lee, A., and Derynck, R. (1994) *J Cell Biol* **126**, 1595-1609.

26. Sampath, T. K., Maliakal, J. C., Hauschka, P. V., Jones, W. K., Sasak, H., Tucker, R. F., White, K. H., Coughlin, J. E., Tucker, M. M., Pang, R. H., and et al. (1992) *J Biol Chem* **267**, 20352-20362.
27. Luppen, C. A., Blake, C. A., Ammirati, K. M., Stevens, M. L., Seeherman, H. J., Wozney, J. M., and Bouxsein, M. L. (2002) *J Bone Miner Res* **17**, 301-310
28. Pereira, R. C., Delany, A. M., and Canalis, E. (2002) *Bone* **30**, 685-691
29. Gori, F., Thomas, T., Hicok, K. C., Spelsberg, T. C., and Riggs, B. L. (1999) *J Bone Miner Res* **14**, 1522-1535.
30. Lee, K. S., Kim, H. J., Li, Q. L., Chi, X. Z., Ueta, C., Komori, T., Wozney, J. M., Kim, E. G., Choi, J. Y., Ryoo, H. M., and Bae, S. C. (2000) *Mol Cell Biol* **20**, 8783-8792.
31. Held, P. G. (2001), Lab Division Applications Detail. <http://www.biotek.com>
32. Kato, Y., Boskey, A., Spevak, L., Dallas, M., Hori, M., and Bonewald, L. F. (2001) *J Bone Miner Res* **16**, 1622-1633
33. Boskey, A. L., Spevak, L., Paschalis, E., Doty, S. B., and McKee, M. D. (2002) *Calcif Tissue Int* **71**, 145-154
34. Ducy, P., and Karsenty, G. (1995) *Mol Cell Biol* **15**, 1858-1869
35. Boyd, K. E., Wells, J., Gutman, J., Bartley, S. M., and Farnham, P. J. (1998) *Proc Natl Acad Sci U S A* **95**, 13887-13892
36. Rickard, D. J., Sullivan, T. A., Shenker, B. J., Leboy, P. S., and Kazhdan, I. (1994) *Dev Biol* **161**, 218-228
37. Lecanda, F., Avioli, L. V., and Cheng, S. L. (1997) *J Cell Biochem* **67**, 386-396
38. Shah, O. J., Kimball, S. R., and Jefferson, L. S. (2000) *Am J Physiol Endocrinol Metab* **279**, E74-82
39. Komori, T., Yagi, H., Nomura, S., Yamaguchi, A., Sasaki, K., Deguchi, K., Shimizu, Y., Bronson, R. T., Gao, Y. H., Inada, M., Sato, M., Okamoto, R., Kitamura, Y., Yoshiki, S., and Kishimoto, T. (1997) *Cell* **89**, 755-764
40. Cooper, M. S., Hewison, M., and Stewart, P. M. (1999) *J Endocrinol* **163**, 159-164
41. Prince, M., Banerjee, C., Javed, A., Green, J., Lian, J. B., Stein, G. S., Bodine, P. V., and Komm, B. S. (2001) *J Cell Biochem* **80**, 424-440
42. Pereira, R. M., Delany, A. M., and Canalis, E. (2001) *Bone* **28**, 484-490.
43. Lee, M. H., Kim, Y. J., Kim, H. J., Park, H. D., Kang, A. R., Kyung, H. M., Sung, J. H., Wozney, J. M., and Ryoo, H. M. (2003) *J Biol Chem*, in press.

FIGURE LEGENDS

FIG. 1. Effect of chronic GC and BMP-2 treatments on calcium accumulation.

MC3T3-E1 cells were chronically treated with 1 μ M DEX starting on day 3 and/or rhBMP-2 (10 or 100 ng/ml) starting on day 5. **(A) Top:** Schematic illustration of experimental protocol. **Bottom:** Alizarin red staining of cultures on day 14. **(B)** Calcium levels in acid extracts of cell layers on days 8-14. The calcium values are corrected for DNA measured in the same extracts. Mean \pm SD (n=3). The letter *U* indicates undetectable levels of calcium. Statistically significant differences ($p < 0.05$) are denoted by *a* when compared to control and by *b* when compared to DEX alone.

FIG. 2. Effect of brief BMP-2 administration on calcium accumulation in cultures

treated chronically with GCs. MC3T3-E1 cells were cultured in the absence (control) or presence of 1 μ M DEX starting on day 3. rhBMP-2 (10 or 100 ng/ml) or vehicle (serum-free media) was briefly added to the cultures on day 5. At the end of the short rhBMP-2 treatment, the medium was removed, the cultures were washed with PBS and fresh DEX-containing medium was added. **(A) Top:** Schematic illustration of the experimental protocol. **Bottom:** Alizarin red staining of day 14-cultures that were treated on day 5 with 100 ng/ml rhBMP-2 or vehicle for a period of 0.25-12 hours as indicated. **(B)** Alizarin red staining of day 14-cultures that were treated on day 5 for ten hours with either 10 or 100 ng/ml of rhBMP-2. **(C)** Calcium levels in acid extracts of cell layers on days 8-14. The calcium values are corrected for DNA measured in the same extracts. Mean \pm SD (n=3). The letter *U* indicates undetectable levels of calcium. Statistically

significant differences ($p < 0.05$) are denoted by *a* when compared to control and by *b* when compared to DEX alone. **(D)** Representative FTIR spectra of cultures treated with vehicle, DEX, or DEX plus 100 ng/ml rhBMP-2. I, II, and III represent the amide I, phosphate ν_1 , ν_3 , and phosphate ν_2 bands, respectively.

FIG. 3. Effect of prolonged and short-term BMP-2 treatment on collagen accumulation, mineral-to-matrix ratio and culture morphology in GC-inhibited cultures. MC3T3-E1 cells were treated with 1 μ M DEX starting on day 3 and rhBMP-2, either 10 or 100 ng/ml, was added on day 5 for either ten hours (*S*, *short*) or 9 days (*P*, *prolonged*). **(A)** Collagen per DNA on days 6, 10 and 14 (top panel). The DNA levels are shown in the bottom panel. **(B)** Mineral-to-matrix ratios in day 14-cultures as determined by FTIR. The ratio of the integrated areas of the phosphate ν_1 , ν_3 band to the amide I band is linearly related to the mineral content (ash weight) of the specimen. **(C)** Bright-field micrographs of day 10-cultures that were treated on day 5 with rhBMP-2 at the indicated concentrations for 10 hours (original magnification 200x). In **(A)** and **(B)**, the bars represent the mean \pm SD of triplicate cultures. However, in Panel **(B)**, the DEX cultures exposed to short-term 10 ng/ml rhBMP-2 did not have sufficient material for FTIR; thus, the triplicate samples were combined. Statistically significant differences ($p < 0.05$) are denoted by *a* when compared to control, by *b* when compared to DEX alone and by *c* when short term rhBMP-2 is compared to prolonged treatment for the same rhBMP-2 and DEX dose.

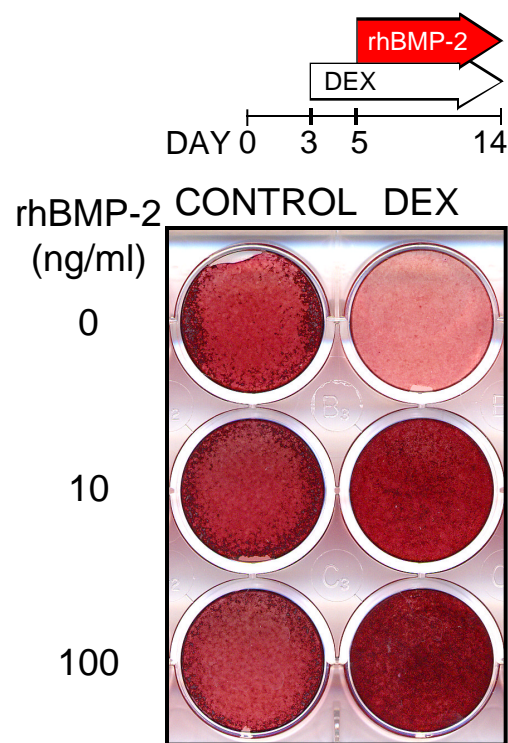
FIG. 4. Effect of prolonged and short-term BMP-2 treatment on alkaline phosphatase activity in GC-inhibited cultures. MC3T3-E1 cells were treated with 1 μ M DEX starting on day 3 and rhBMP-2, either 10 or 100 ng/ml, was added on day 5 for either ten hours (*S, short*) or 9 days (*P, prolonged*). Mean \pm SD (n=3). Statistically significant differences ($p < 0.05$) are denoted by *a* when compared to control, by *b* when compared to DEX alone and by *c* when short term rhBMP-2 is compared to chronic treatment for the same rhBMP-2 and DEX dose.

FIG. 5. Effect of GCs and BMP-2 on Runx2 DNA-binding activity. MC3T3-E1 cells were treated with 1 μ M DEX on day 3 and 100 ng/ml rhBMP-2 on day 5. **(A)** Runx2 EMSA was performed 2, 21 or 42 hours after administration on day 3 of fresh medium containing DEX or ethanol vehicle. **(B)** Runx2 EMSA was performed on day 5, after short exposure (0.5-10 hours) to either 100 ng/ml rhBMP-2 or medium vehicle. **(C)** Identification of the main complex as Runx2. Runx2 EMSA of a control culture was performed without competition; in the presence of a wild-type unlabeled Runx2-binding oligonucleotide (*WT*); in the presence of a similar oligonucleotide that bears a mutation at the Runx2 binding site (*MT*); and in the presence of Runx2 antibodies (*Ab*). In the second lane from the right, the *Ab* were incubated with the probe in the absence of cell extract. **(D)** Northern analysis of osteocalcin mRNA in cultures treated with DEX as in Panel A for 2, 5 and 21 hours. The ethidium bromide-stained gel is shown to demonstrate equal loading.

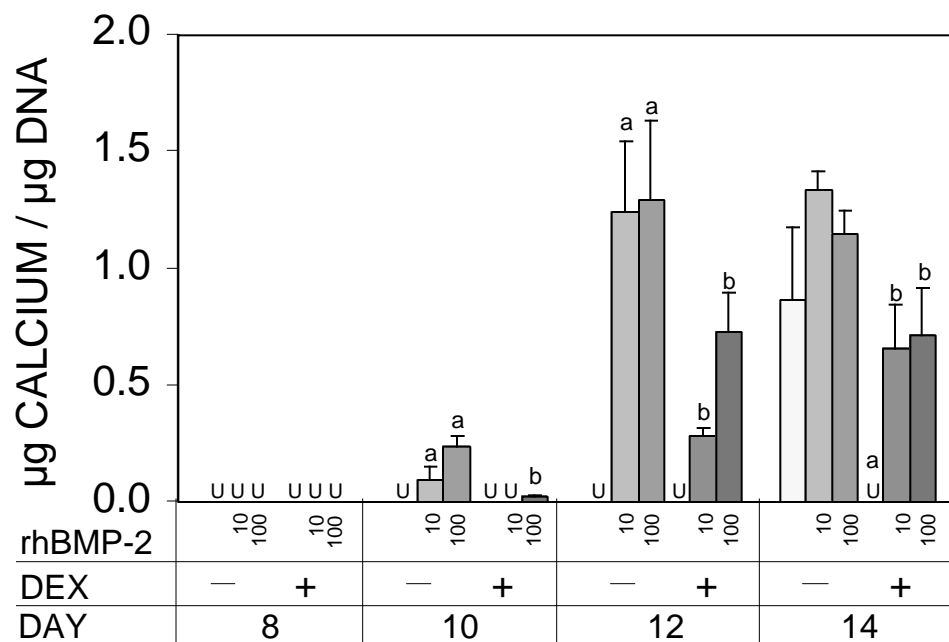
FIG. 6. Effect of GCs and BMP-2 on Runx2 transcriptional activity. MC3T3-E1 cells were transfected with the indicated constructs and treated with DEX and/or rhBMP-2 as indicated. Luciferase activity was measured on day 6. Mean \pm SD (n=3). Statistically significant differences ($p < 0.05$) are denoted by *a* when compared to control and by *b* when compared to DEX alone. *Inset*: Representative RT-PCR showing endogenous osteocalcin (OC) and 18S RNA in parallel cultures.

FIG. 7. Effect of GC on Runx2 association with the osteocalcin promoter in living cells. MC3T3-E1 cultures were treated for 48 hours with 1 μ M DEX, starting on day 3, 5, or 7 and subjected to chromatin immunoprecipitation with Runx2 antibodies. Purified DNA was PCR-amplified with primers corresponding to promoter sequences of the osteocalcin (*O*) gene flanking the Runx2-binding site at position -138. An insulin (*I*) promoter fragment was amplified as control. Genomic DNA was amplified to demonstrate comparable amplification efficiency for the two promoter fragments. All PCR reactions were performed within a close-to-linear range. Figure shows ethidium bromide-stained 1% agarose gel with results from one representative of two experiments.

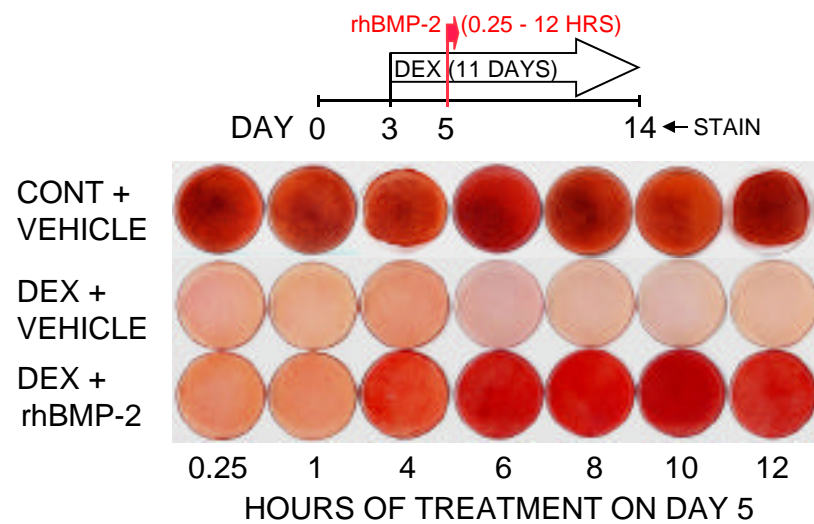
FIG. 8. Effect of GCs and BMP-2 on cell cycle progression. MC3T3-E1 cells were treated with 1 μ M DEX on day 3 and rhBMP-2 (100 ng/ml) was added on day 5 either (A) with medium change, to simulate the chronic exposure protocol, or (B) without medium change, to simulate the short-term exposure protocol. The percentages of cells in the S and G2/M phases of the cell cycle were determined every 3 hours between 10 and 37 hours after administration of rhBMP-2.



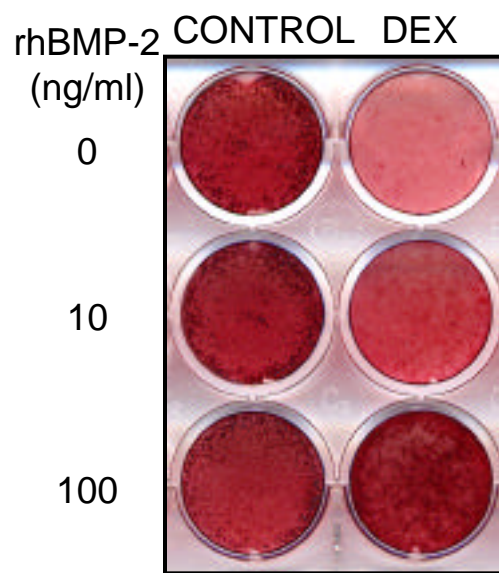
Luppen et al, Figure 1A



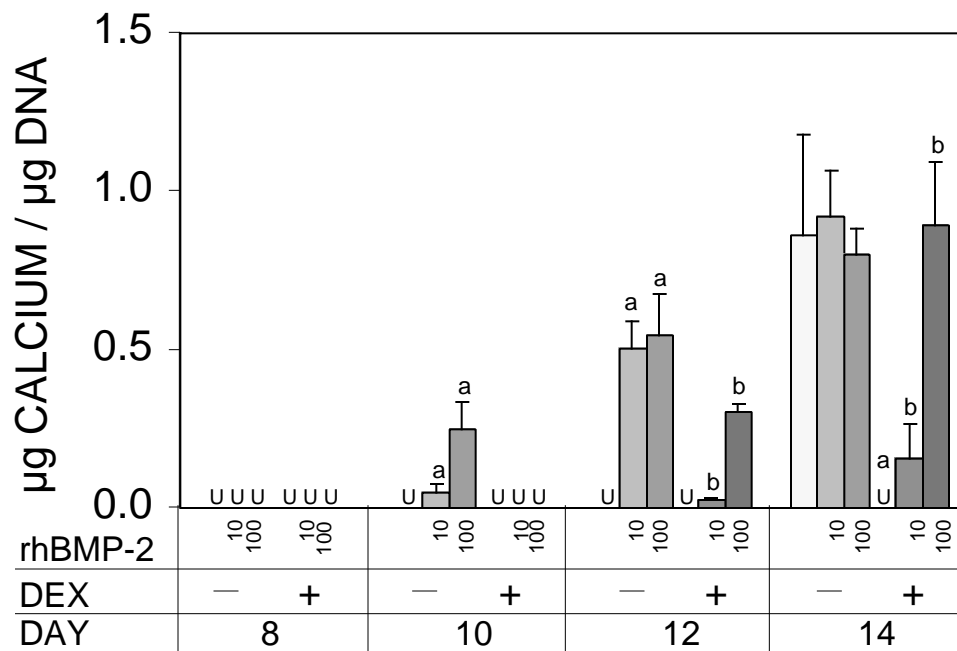
Luppen et al, Figure 1B



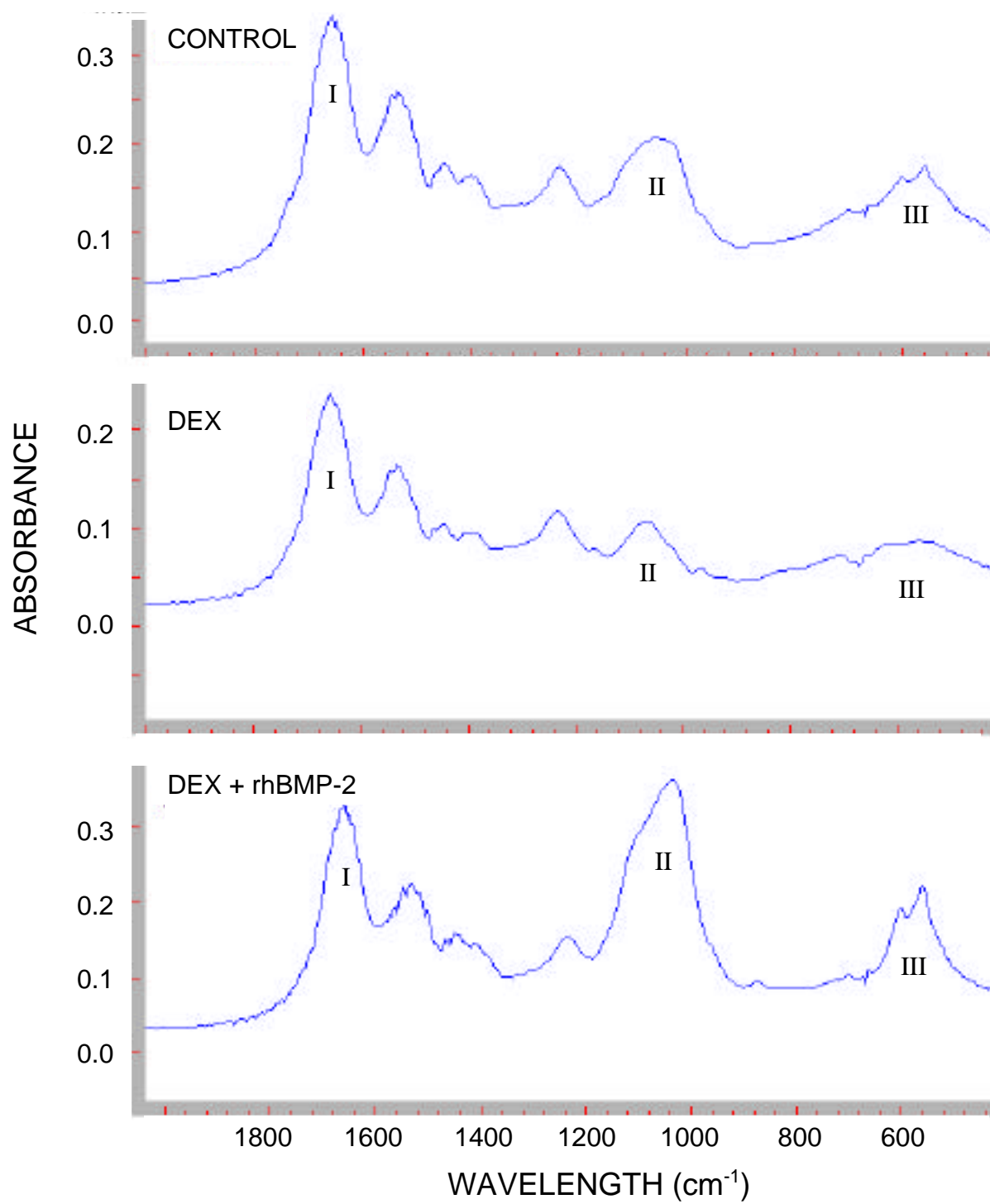
Luppen et al, Figure 2A



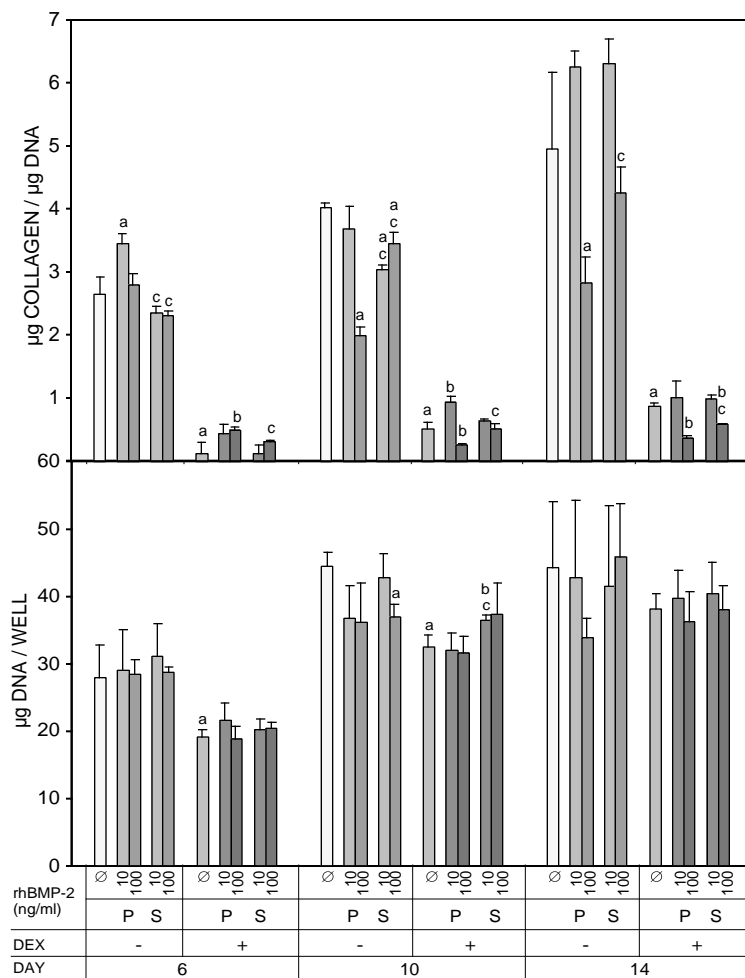
Luppen et al, Figure 2B



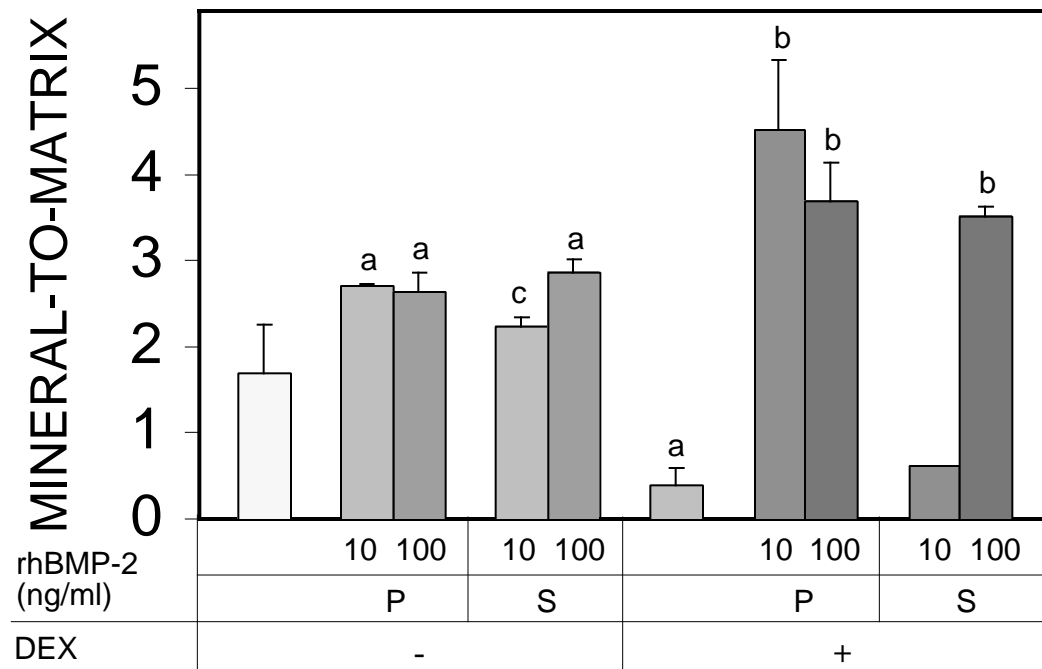
Luppen et al, Figure 2C



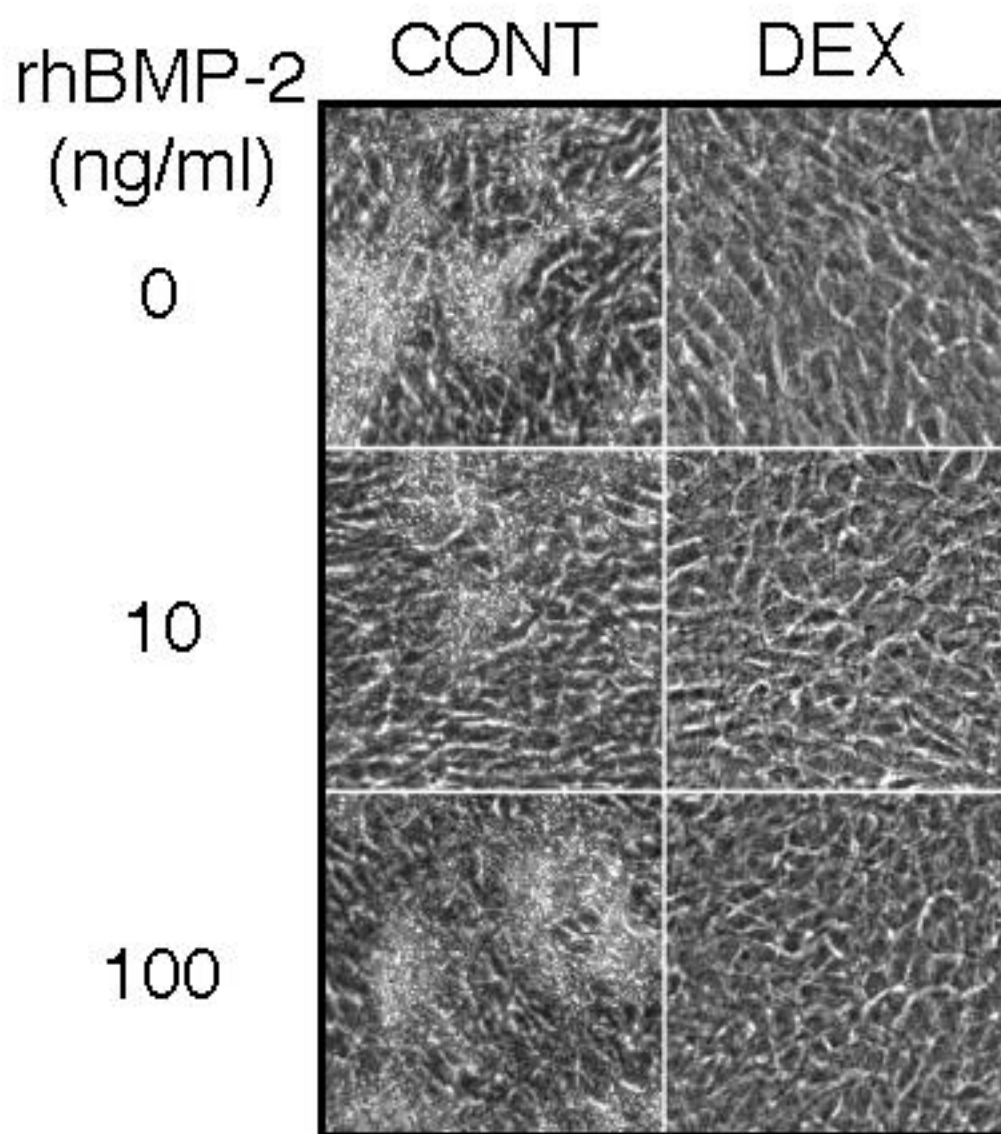
Luppen et al, Figure 2D



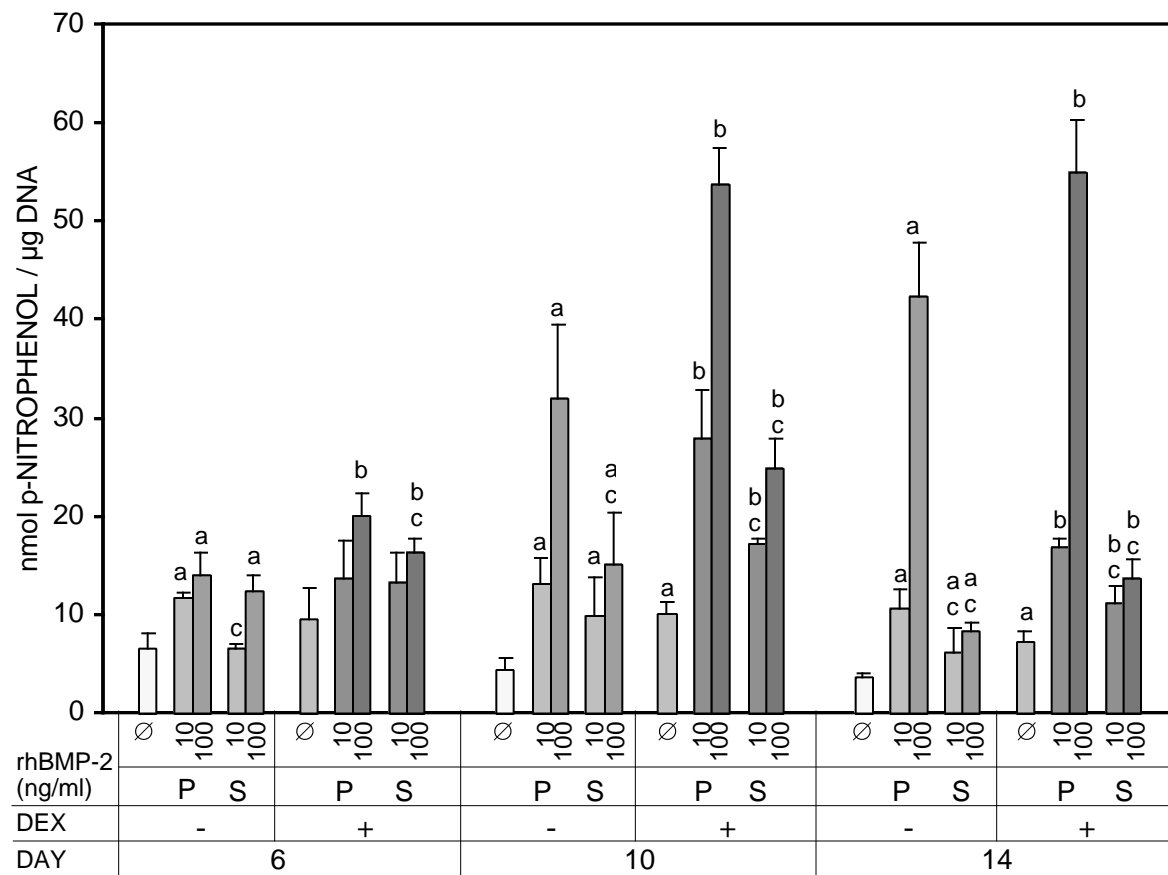
Luppen et al, Figure 3A



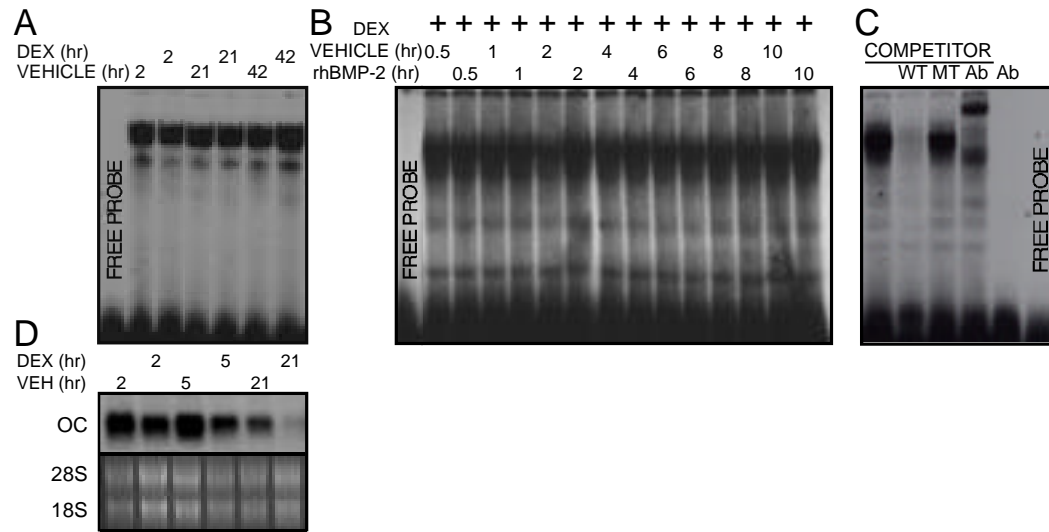
Luppen et al, Figure 3B



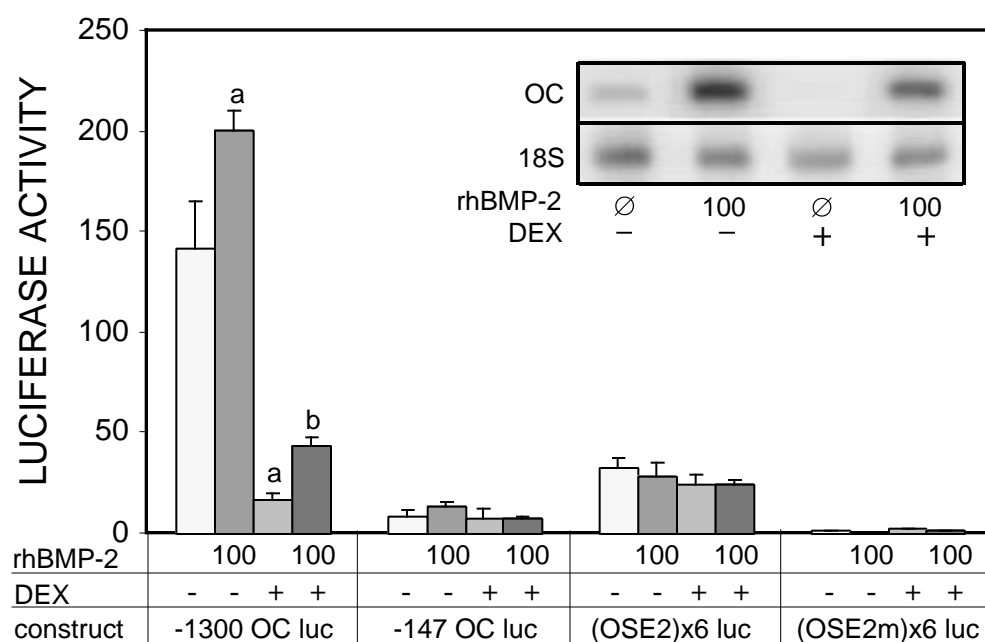
Luppen et al, Figure 3C



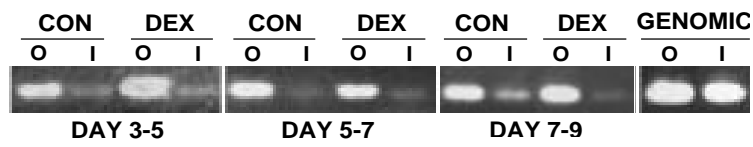
Luppen et al, Figure 4



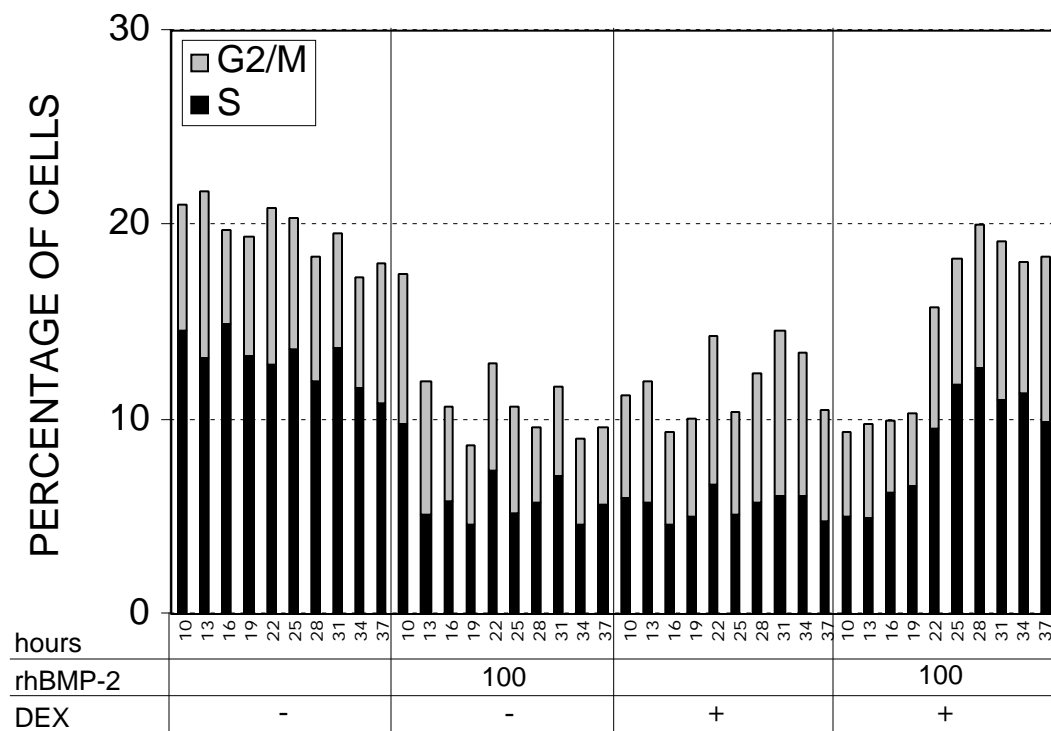
Luppen et al, Figure 5



Luppen et al, Figure 6



Luppen et al Figure 7



Luppen et al, Figure 8B

Brief rhBMP-2 treatment of glucocorticoid-inhibited MC3T3-E1 osteoblasts rescues commitment-associated cell cycle and mineralization without alteration of Runx2

Cynthia A. Luppen, Nathalie Leclerc, Tommy Noh, Artem Barski, Arvinder Khokhar,
Adele L. Boskey, Elisheva Smith and Baruch Frenkel

J. Biol. Chem. published online August 20, 2003

Access the most updated version of this article at doi: [10.1074/jbc.M306730200](https://doi.org/10.1074/jbc.M306730200)

Alerts:

- [When this article is cited](#)
- [When a correction for this article is posted](#)

[Click here](#) to choose from all of JBC's e-mail alerts